Graphene-based polaritonic crystal

Yu. V. Bludov, N. M. R. Peres, and M. I. Vasilevskiy
Centro de Física e Departamento de Física, Universidade do Minho, Campus de Gualtar, Braga 4710-057, Portugal
(Received 17 April 2012; published 5 June 2012)

It is shown that monolayer graphene deposited on a spatially periodic gate behaves as a polaritonic crystal. Its band structure depending on the applied gate voltage is studied. The scattering of electromagnetic radiation from such a crystal is presented calculated and its spectral dependence is analyzed in terms of Fano-type resonances between the reflected continuum and plasmon-polariton modes forming narrow bands.

DOI: 10.1103/PhysRevB.85.245409 PACS number(s): 81.05.ue, 72.80.Vp, 78.67.Wj

I. INTRODUCTION

Coupling of light to the surface charges at a metal-dielectric interface gives rise to a special kind of evanescent electromagnetic (EM) waves called surface plasmon-polaritons (SPPs).[1] The specific properties of SPPs allow for their use in variety of practical applications. The sensitivity of SPPs to the properties of the dielectric, the metal, and the interface is used in SPP-based sensors[2,3] and in high-resolution imaging.[4–6] Surface plasmons give rise to very large EM fields at the surface, which is important for surface-enhanced optical spectroscopies.[7] Moreover, the SPP wavelength can be much smaller than the photon wavelength, opening the possibility for further miniaturization of photonics components, a new field of research called *nanoplasmonics*.[8] Of particular interest is the ability to tune SPP modes in plasmonic devices by external control: using an electric field in a liquid crystal,[9] a magnetic field in a magneto-optically active substrate,[10] thermal heating,[11] or a light beam focused on a nonlinear coating.[12]

The possibility of tuning the amount of free carriers in graphene using an external gate allows for an effective control of the material's optical properties.[13–16] Exploring graphene, a tunable two-dimensional (2D) metal, for plasmonics at the nanoscale reveals new physical effects and opens exciting possibilities in this field.[17–20] When compared to their counterparts in conventional 2D electron systems, SPPs in graphene exhibit some new and unusual properties, such as the $1/4$-power density dependence of the SPP frequency[17] and the existence of s-polarized waves.[18] Moreover, SPPs in graphene can potentially be used in a variety of practical applications. For example, using the amplification of SPPs in graphene opens the possibility to create a terahertz radiation source;[21] employing the attenuated total reflection (ATR) configuration with a gated graphene layer allows for a resonant switching of the reflection coefficient of an external EM wave from nearly unity to almost zero.[22]

Recently, a new class of metamaterials with a high potential interest for transformation optics was proposed, based on SPPs in graphene, either deposited on a uneven surface[23] or composed of an array of microribbons.[24] When SPPs propagate along a periodically modulated surface, the concept of a "surface polaritonic crystal" can be introduced,[5] where the SPP dispersion shows a band-gap structure,[25] in analogy with a photonic crystal. In this paper we propose and theoretically analyze a different type of SPP crystal, based on a graphene sheet deposited on top of a periodically modulated gate electrode (wafer), as schematically represented in Fig. 1(a). Using graphene as a polaritonic crystal opens the possibility of tuning the positions and the widths of the gaps in the spectrum as well as the plasmonic resonance frequencies. This can be done not during the fabrication process (as in Ref. 26), but dynamically, by varying gate voltage applied to graphene.

The paper is organized as follows. In Sec. II we describe the model of the polaritonic crystal and derive expressions for the SPP dispersion relation and for the reflectivity of this structure. In Sec. III we discuss the general properties of SPPs in a graphene-based polaritonic crystal as well as the details of SPP excitation via an external electromagnetic wave, with and without the prism. Finally, in Sec. IV, the main results of the paper are summarized.

II. ELECTROMAGNETIC WAVES IN MONOLAYER GRAPHENE DEPOSITED ON A PERIODICALLY MODULATED GATE

In order to achieve the periodic modulation of graphene's conductivity, we consider a single graphene layer in the plane $z = 0$ deposited on a SiO_2 substrate with a dielectric constant ε_1 [see Fig. 1(a)]. The opposite side of the substrate has a periodic relief with a spatial period D, such that $h(x) = h(x + D)$. To be specific, we will consider the dielectric thickness modulation of the form $h(x) = h_0[1 + a\cos(gx)]$, where a is the modulation depth and $g = 2\pi/D$. A conductive wafer is placed beneath this modulated surface, serving as a gate contact. If a constant gate voltage V is applied between the graphene layer and the wafer, a periodic modulation of the graphene conductivity can be achieved. If $D \gg h(x)$, the carrier density in graphene can be expressed as $n(x) = \xi\varepsilon_1 V/4\pi e h(x)$, where e is the electron charge and ξ is a coefficient between 1 and 2 depending on the charge distribution in the corrugated gate electrode (further in the paper we use $\xi = 1$). Owing to the periodicity of the surface relief, the carrier density in graphene is a periodic function with the same period D, thus resulting in the periodicity of its optical conductivity, $\sigma(x,\omega) = \sigma(x + D,\omega)$. The latter can be related to the local value of the chemical potential counted with respect to the Dirac point, $\mu(x) = \hbar v_F\{\pi n(x)\}^{1/2}$, where v_F is the Fermi velocity.

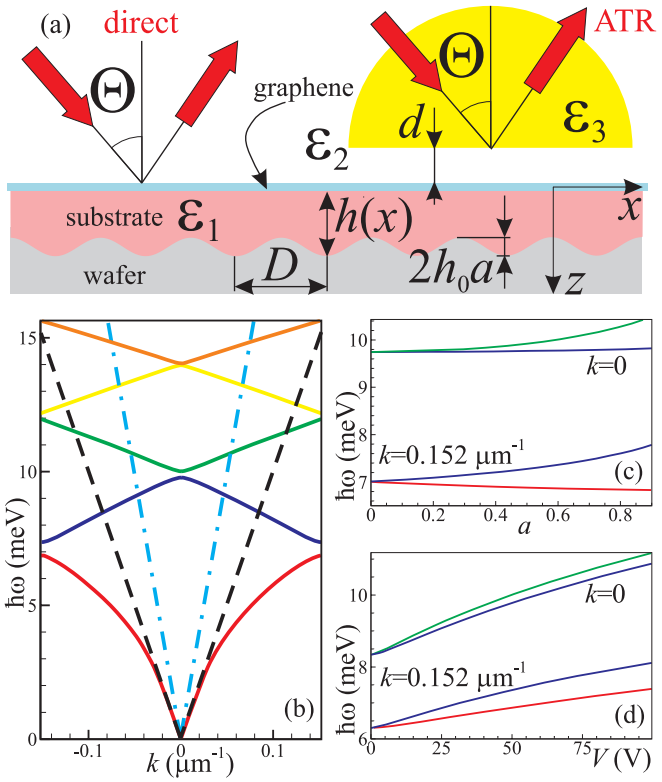

FIG. 1. (Color online) (a) Geometry of the system: "Sandwich-like" structure containing a graphene layer on a substrate composed of a dielectric spacer (with dielectric constant ε_1) and a transparent conductive wafer with a periodic interface relief. (b) Real part of the SPP frequency versus wave vector in the first Brillouin zone, calculated for a single graphene layer at interface of two semi-infinite dielectric media. (c),(d) Edges of the first two lowest gaps (at edge and at center of Brillouin zone) versus modulation depth a (c) or gate voltage V (d). The parameters are the following: $\varepsilon_2 = 1$, $\varepsilon_1 = 3.9$, $h_0 = 300$ nm, $D = 20.67$ μm, $a = 0.6$ (b) and (d). In panels (b) and (c) $V = 50$ V, corresponding to an average chemical potential $\bar{\mu} \approx 0.222$ eV. In panel (b) the light lines for the cladding media, $kc/\omega = \sqrt{\varepsilon_m}$, are shown dashed ($m = 1$) and dash-dotted ($m = 2$).

As it is shown below, the periodic modulation of the optical conductivity leads to the possibility of direct coupling of a propagating EM wave to the surface plasmons [Fig. 1(a), left, where ε_2 is the dielectric constant of the medium above graphene]. However, only those SPP modes which lie within the light cone, $\omega/k = c/\sqrt{\varepsilon_2}$, shown by dash-dotted lines in Fig. 1(b), can be excited this way. In general, for the SPP excitation one has to consider an ATR structure like the one described in Ref. 22, which includes a prism with a dielectric constant ε_3 [Fig. 1(a), right]. Usually there is a gap between the graphene sheet and the prism, which we shall model as a dielectric layer of a thickness d and a dielectric constant ε_2. We assume that the prism occupies the half space $z < -d$ and a p-polarized EM wave impinges on the boundary $z = -d$, coming from $z = -\infty$ at an angle of incidence Θ.

Since the dielectric properties of the structure are periodic along x, the solution of Maxwell's equations, $\mathrm{rot}\mathbf{E}^{(m)} = i\kappa\mathbf{H}^{(m)}$, $\mathrm{rot}\mathbf{H}^{(m)} = -i\kappa\varepsilon_m\mathbf{E}^{(m)}$ for the p-polarized wave [with components $\boldsymbol{E} = (E_x, 0, E_z)$ and $\boldsymbol{H} = (0, H_y, 0)$] can be written as Fourier-Floquet series:

$$H_y^{(m)}(x,z) = \sum_{n=-\infty}^{\infty} \left[A_n^{(m)} \exp\left(\kappa q_n^{(m)} z\right) + B_n^{(m)} \exp\left(-\kappa q_n^{(m)} z\right)\right] \exp[i(k+ng)x], \quad (1)$$

$$E_x^{(m)}(x,z) = \sum_{n=-\infty}^{\infty} \frac{q_n^{(m)}}{i\varepsilon_m} \left[A_n^{(m)} \exp\left(\kappa q_n^{(m)} z\right) - B_n^{(m)} \exp\left(-\kappa q_n^{(m)} z\right)\right] \exp[i(k+ng)x]. \quad (2)$$

In Eqs. (1) and (2), $q_n^{(m)} = \sqrt{[(k+ng)/\kappa]^2 - \epsilon_m}$ is the in-plane component of the photon wave vector in the medium m ($m = 1,2,3$; $m = 3$ applies only for the ATR configuration), $\kappa = \omega/c$, and c is the speed of light in vacuum. Although the substrate is finite, for simplicity we shall consider the medium 1 as semi-infinite in the wave equations. If the gate electrode is transparent, this simplification is not crucial for the analysis of the optical properties of the modulated structure. Boundary conditions at $z = -d$ imply the continuity of the tangential components of the electric and magnetic fields, $[E_x^{(3)}(x, -d) = E_x^{(2)}(x, -d)$, $H_y^{(3)}(x, -d) = H_y^{(2)}(x, -d)]$. At $z = 0$, the tangential component of the electric field is continuous, $E_x^{(1)}(x,0) = E_x^{(2)}(x,0)$, while the discontinuity of the tangential component of the magnetic field, $H_y^{(1)}(x,0) - H_y^{(2)}(x,0) = -(4\pi/c)j_x = -(4\pi/c)\sigma(x,\omega)E_x(x,0)$, stems from the presence of surface currents (caused by the SPP electric field) in the graphene layer. Applying these boundary conditions, one can find the explicit form of the transfer matrices, $\hat{M}^{m\leftarrow m+1}$, which relate the coefficients in Eqs. (1) and (2) for different m, $(\ldots, A_n^{(m)}, B_n^{(m)}, A_{n+1}^{(m)}, B_{n+1}^{(m)}, \ldots)^T = \hat{M}^{m\leftarrow m+1}(\ldots, A_n^{(m+1)}, B_n^{(m+1)}, A_{n+1}^{(m+1)}, B_{n+1}^{(m+1)}, \ldots)^T$. The matrices $\hat{M}^{m\leftarrow m+1}$ consist of 2×2 blocks $\hat{M}_{n,l}^{m\leftarrow m+1}$,

$$\hat{M}_{n,l}^{1\leftarrow 2} = \frac{1}{2}\begin{pmatrix} Q_{n,l}^{(1,+)} - \frac{4\pi q_n^{(2)}}{ic\varepsilon_2}\sigma_{n-l} & Q_{n,l}^{(1,-)} + \frac{4\pi q_n^{(2)}}{ic\varepsilon_2}\sigma_{n-l} \\ Q_{n,l}^{(1,-)} - \frac{4\pi q_n^{(2)}}{ic\varepsilon_2}\sigma_{n-l} & Q_{n,l}^{(1,+)} + \frac{4\pi q_n^{(2)}}{ic\varepsilon_2}\sigma_{n-l} \end{pmatrix},$$

$$\hat{M}_{n,l}^{2\leftarrow 3} = \frac{1}{2}\begin{pmatrix} Q_{n,l}^{(2,+)} e^{\kappa[q_l^{(2)} - q_l^{(3)}]d} & Q_{n,l}^{(2,-)} e^{\kappa[q_l^{(2)} + q_l^{(3)}]d} \\ Q_{n,l}^{(2,-)} e^{-\kappa[q_l^{(2)} + q_l^{(3)}]d} & Q_{n,l}^{(2,+)} e^{-\kappa[q_l^{(2)} - q_l^{(3)}]d} \end{pmatrix},$$

where $Q_{n,l}^{(m,\pm)} = \delta_{n,l}\left(1 \pm F_n^{(m)}\right)$, $F_n^{(m)} = \varepsilon_m q_n^{(m+1)}/\varepsilon_{m+1} q_n^{(m)}$, $\delta_{n,l}$ is a Kronecker symbol, $\sigma_n = D^{-1}\int_0^D \sigma(x,\omega)\exp(-ingx)dx$ is the spatial Fourier harmonic of the graphene conductivity.

The meaning of the coefficients $A_n^{(m)}$, $B_n^{(m)}$ is different for the different media. The waves corresponding to the different terms in Eqs. (1) and (2) can be either propagating [with $\mathrm{Im}(q_n^{(m)}) < 0$] or evanescent [with $\mathrm{Re}(q_n^{(m)}) > 0$]. Since the incident wave in the medium 3 possesses only the $n = 0$ component (zero harmonic), $\mathrm{Im}(q_0^{(3)}) < 0$ and the coefficients $B_n^{(3)} = \delta_{n,0} H_i \exp(-\kappa q_0^{(3)} d)$ are proportional to the magnetic-field amplitude (H_i) in the incident wave. In the medium 1, the coefficients $A_n^{(1)} \equiv 0$ correspond to the absence of the corresponding harmonics coming from $z = \infty$. Then, multiplying the matrices $\hat{M}^{1\leftarrow 2}\hat{M}^{2\leftarrow 3}$, and taking into account the block-diagonal structure of the matrix $\hat{M}^{2\leftarrow 3}$, after some algebra we obtain the following equations for the amplitudes

of the reflected harmonics, $r_n = A_n^{(3)} \exp(-\kappa q_n^{(3)} d)$:

$$\hat{R} \times (\ldots, r_n, r_{n+1}, \ldots)^T = (\ldots, H_{n'}^i, H_{n'+1}^i, \ldots)^T, \quad (3)$$

where the elements of the matrix $\hat{R}$ and the vector H_n^i are

$$R_{n,n'} = \left[\delta_{n,n'} F_n^{(1)} - \frac{4\pi q_{n'}^{(2)} \sigma_{n-n'}}{ic\varepsilon_2}\right]\left[S_{n'} + F_{n'}^{(2)} C_{n'}\right] + \delta_{n,n'}\left[C_{n'} + F_{n'}^{(2)} S_{n'}\right], \quad (4)$$

$$H_n^i = -\left\{\left[\delta_{n,0} F_0^{(1)} - \frac{4\pi q_0^{(2)} \sigma_n}{ic\varepsilon_2}\right]\left[S_0 - F_0^{(2)} C_0\right] + \delta_{n,0}\left[C_0 + F_0^{(2)} S_0\right]\right\} H_i, \quad (5)$$

with $C_n = \cosh(\kappa q_n^{(2)} d)$ and $S_n = \sinh(\kappa q_n^{(2)} d)$.

III. RESULTS AND DISCUSSION

In order to obtain the general properties of SPPs in graphene with periodically modulated conductivity, we first consider the eigenvalue problem for the matrix $\hat{R}$ leading to the dispersion relation for SPPs in a flat 2D graphene layer placed between two lossless dielectric media (ε_1 and ε_2). We put $\varepsilon_3 = \varepsilon_2$ and solve the equation $\det(\hat{R}) = 0$. It yields complex eigenvalues because the graphene conductivity $\sigma(x,\omega)$ has both real and imaginary parts, therefore the SPP eigenmodes are dissipative. The SPP dispersion curve for the real part of the frequency eigenvalue, ω, vs wavenumber for the first Brillouin zone, $k \in [-g/2, g/2]$, is presented in Fig. 1(b). The imaginary part of the frequency (mode damping) is an order of magnitude smaller than ω. As it can be seen from Fig. 1(b), the SPP dispersion curve is periodic in the k space, with the period g. There are bands of allowed SPP frequencies, separated by gaps opening at the edges and in the center of the Brillouin zone, where SPPs do not exist. As expected, the widths of the gaps increase with the increase of the modulation depth a [Fig. 1(c)]. A natural question arises: *is it possible to control dynamically the gap widths through some nondestructive external knob?* The positive answer to this question is evident from Fig. 1(d). Since the chemical potential of graphene can be tuned by the gate voltage, one can shift the spectral position and width of the gaps by changing V. Therefore the SPP crystal band structure can be controlled dynamically.

Another feature of the SPP spectrum in periodically modulated graphene is that the "scan line," $k = \kappa\sqrt{\varepsilon_2}\sin\Theta$, located within the dash-dotted lines in Fig. 1(b) crosses the SPP dispersion curves. This situation is completely different from the case of uniform graphene,[22] where both phase and group velocities of SPPs are smaller than the velocities of light in the surrounding dielectrics. SPPs in periodically modulated graphene can be excited by an external propagating EM wave, without an ATR prism. This is illustrated by Fig. 2, where the amplitudes of the reflected field harmonics are presented; they have been calculated by solving Eq. (3) for $d = 0$ and $\varepsilon_3 = \varepsilon_2$ (in this case, ω is real).

At normal incidence ($\Theta = 0$), the zero harmonic reflection coefficient of the SPP crystal exhibits just one maximum at $\hbar\omega \approx 10$ meV [see Figs. 2(a) and 2(b)], which approximately corresponds to the upper edge of the second gap in Fig. 1(b). This is related to the parity of the SPP mode with respect

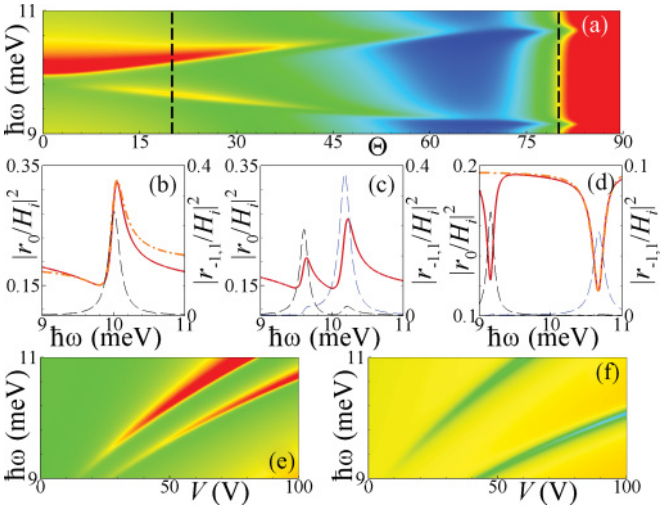

FIG. 2. (Color online) (a) Zero harmonic reflection coefficient $|r_0/H_i|^2$ vs frequency and incidence angle for SPPs in periodically modulated graphene with $V = 50$ V. (b)–(d) Zero harmonic reflection coefficient (red solid lines) and relative square amplitudes, $|r_n/H_i|^2$, of $n = 1$ (blue dashed lines) and $n = -1$ (black dashed lines) harmonics for the incidence angles $\Theta = 0^\circ$ (b), $\Theta = 20^\circ$ (c), and $\Theta = 80^\circ$ (d) [the latter two correspond to the vertical dashed lines in panel (a)]. (e),(f) Zero harmonic reflection coefficient vs frequency and gate voltage for $\Theta = 20^\circ$ (e) and $\Theta = 80^\circ$ (f). Other parameters are the same as in Fig. 1. In panels (a), (e), and (f) red (blue) color corresponds to high (low) values of the reflection coefficient. In panels (b) and (d) Fano-type fits are shown by dash-dotted (orange) lines, with $R_0 = 0.1508$, $\delta R = 0.035$, $q = 2$, $\hbar\omega_0 = 10$ meV (b) and $R_0 = 0.116$, $\delta R = 0.08$, $q = 0.08$, $\omega_0 = 10.68$meV (d); $\hbar\gamma = 0.1$ meV.

to $x = 0$, since it is excited by a plane wave and $h(x)$ is an even function. Also from Fig. 2(b) it is clearly seen that the enhanced reflection of the zero harmonic corresponds to the excitation of the SPP harmonics with $n = -1$ and $n = 1$. They correspond to the bottom of the third allowed SPP band and, for normal incidence, are mixed into the $k = 0$ band bottom mode. For oblique incidence [Figs. 2(c)–2(f)], there are *two* resonances corresponding to the second and third SPP bands and producing reflected field harmonics with $n = \pm 1$. SPPs are effectively excited when the frequency and the in-plane component of the wave vector of the incident EM wave match those of SPP eigenmodes of the modulated graphene. The energy of the incident wave is transferred into the SPP harmonics with $n = \pm 1$, while the reflected wave in the far field contains only zero harmonic. Note that the position and the amplitude of the resonances can be controlled by changing the gate voltage [Figs. 2(e) and 2(f)]. Quite interestingly, the direct excitation of $n = \pm 2$ and higher SPP bands can produce *propagating* EM waves with $|k \pm g| \leqslant \kappa\sqrt{\varepsilon_2}$, scattered at angles

$$\Theta_{\pm 1} = \arcsin\left(\frac{k \pm g}{\kappa\sqrt{\varepsilon_2}}\right).$$

Let us focus on the characteristic spectral dispersion of the zero harmonic reflection coefficient around each of the SPP resonance frequencies [Figs. 2(b) and 2(c)] where an intrinsic mode of the SPP crystal is excited. This is an asymmetric

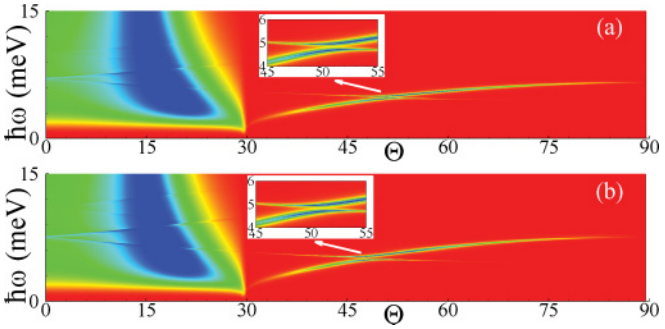

FIG. 3. (Color online) Reflection coefficient of zero harmonic $|r_0/H_i|^2$ vs frequency ω and angle of incidence Θ for ATR excitation of SPPs in graphene with parameters $\varepsilon_3 = 16$, $\varepsilon_2 = 1$, $\varepsilon_1 = 3.9$, $h_0 = 300$ nm, $D = 10.34$ μm, $a = 0.6$, $d = 10$ μm, $V = 50$ V (a), or 90 V (b).

Fano-type resonance with a maximum accompanied by a neighboring minimum. a phenomenon first discovered in the ionization spectra[27] of He and now known in many different branches of physics including light scattering by photonic crystals.[28] If a discrete mode couples to a continuum of excitations, the Fano resonance arises from the constructive (destructive) interference of the localized and delocalized waves, taking place above (below) the discrete mode frequency ω_0. A simple analytic expression to describe such a line shape was suggested by Fano:[27]

$$F(\omega) = \frac{(q\gamma + \omega - \omega_0)^2}{(\omega - \omega_0)^2 + \gamma^2}, \tag{6}$$

where γ is the mode damping and q is an asymmetry parameter related to the relative strengths of the transitions associated with the discrete and continuum modes. Figure 2(b) shows a Fano-type fit, $R(\omega) = R_0 + \delta R \cdot F(\omega)$, to the calculated reflectivity spectrum (R_0 and δR are constants). The coupling between the continuum of propagating EM modes in the medium 2 and the SPP Bragg mode of the polaritonic crystal decreases with the increase of the incidence angle. When Θ is close to the Brewster angle, $\Theta_b = \text{atan}(\sqrt{\varepsilon_1/\varepsilon_2}) \approx 63^\circ$, the resonant excitation of $n = \pm 1$ modes results in two narrow and almost symmetric minima in the spectrum [see Fig. 2(d) where the Fano fit corresponds to $q = 0.08$, compared to $q = 2$ in Fig. 2(b)].

As mentioned above, the direct excitation of SPPs by a propagating wave allows for probing only the part of the polaritonic crystal band structure comprised between the dash-dotted light lines in Fig. 1(b). Beyond this, one has to use the ATR scheme where SPPs are excited by an evanescent wave with a sufficiently large wavenumber, $k = \kappa\sqrt{\varepsilon_3}\sin\Theta$. The results calculated for the ATR structure are presented in Fig. 3, where the SPP excitation conditions correspond to a minimum of the zero harmonic reflectance related to the gap between the first and the second SPP bands. The mode anticrossing, corresponding to the edges of the gap, is clearly seen in Figs. 3(a) and 3(b) (near $\Theta \approx 50^\circ$, see insets). Comparison of Figs. 3(a) and 3(b) shows that increasing the gate voltage results in an increase of the gap width, as it could be anticipated from Fig. 1(f).

IV. CONCLUSIONS

To conclude, we have demonstrated that a single graphene layer deposited on a "sandwichlike" structure with a periodically corrugated gate electrode has the properties of a polaritonic crystal, namely, possesses a band structure with gaps that can be tuned by the gate voltage. We showed that electrostatic gating of graphene on top of a substrate with a periodically modulated thickness results in a periodic modulation of the charge-carrier density in graphene which gives rise to a periodic modulation of graphene's conductivity. This crystal exhibits Fano-type resonances in the reflectance coefficient of the reflected EM wave due to the excitation of surface plasmon-polariton Bragg modes. In this kind of crystal, the Fano resonances involving SPPs in graphene can be excited directly (without using a prism) by the incident EM wave upon its diffraction on the periodic modulation of graphene's conductivity.

[1] A. A. Maradudin, *Surface Polaritons. Electromagnetic Waves at Surfaces and Interfaces*, edited by V. M. Agranovich and D. L. Mills (North-Holland, Amsterdam, 1982); H. Räther, *Surface Plasmons on Smooth and Rough Surfaces and on Gratings* (Springer-Verlag, Berlin, 1988).
[2] J. Homola, S. S. Yee, and G. Gauglitz, Sens. Actuators, B **54**, 3 (1999).
[3] A. Shalabney and I. Abdulhalim, Laser Photon. Rev. **5**, 571 (2011).
[4] W. L. Barnes, A. Dereux, and T. W. Ebbesen, Nature (London) **424**, 824 (2003).
[5] A. V. Zayats, I. I. Smolyaninov, and A. A. Maradudin, Phys. Rep. **408**, 131 (2005).
[6] S. Kawata, Y. Inouye, and P. Verma, Nat. Photon. **3**, 388 (2009).
[7] G. V. Hartland and G. Schatz, J. Phys. Chem. C **115**, 15121 (2011).
[8] P. Vasa, C. Ropers, R. Pomraenke, and Ch. Lienau, Laser Photon. Rev. **3**, 483 (2009).
[9] W. Dickson, G. A. Wurtz, P. R. Evans, R. J. Pollard, and A. V. Zayats, Nano Lett. **8**, 281 (2008).
[10] G. A. Wurtz, W. Hendren, R. Pollard, R. Atkinson, L. Le Guyader, A. Kirilyuk, Th. Rasing, I. I. Smolyaninov, and A. V. Zayats, New J. Phys. **10**, 105012 (2008).
[11] O. Tsilipakos, T. V. Yioultsis, and E. E. Kriezisa, J. Appl. Phys. **106**, 093109 (2009); J. Gosciniak, S. I. Bozhevolnyi, Th. B. Andersen, V. S. Volkov, J. Kjelstrup-Hansen, L. Markey, and A. Dereu, Opt. Express **18**, 1207 (2010).
[12] G. A. Wurtz, R. Pollard, and A. V. Zayats, Phys. Rev. Lett. **97**, 057402 (2006).
[13] A. H. Castro Neto, F. Guinea, N. M. R. Peres, K. S. Novoselov, and A. K. Geim, Rev. Mod. Phys. **81**, 109 (2009).
[14] K. S. Novoselov, A. K. Geim, S. V. Morozov, D. Jiang, Y. Zhang, S. V. Dubonos, I. V. Grigorieva, and A. A. Firsov, Science **306**, 666 (2004).

[15] F. Wang, Y. Zhang, C. Tian, C. Girit, A. Zettl, M. Crommie, and Y. R. Shen, Science **320**, 206 (2008); Z. Q. Li, E. A. Henriksen, Z. Jiang, Z. Hao, M. C. Martin, P. Kim, H. L. Stormer, and D. N. Basov, Nat. Phys. **4**, 532 (2008).

[16] F. H. L. Koppens, D. E. Chang, and F. J. Garcia de Abajo, Nano Lett. **11**, 3370 (2011).

[17] O. Vafek, Phys. Rev. Lett. **97**, 266406 (2006); X.-F. Wang and T. Chakraborty, Phys. Rev. B **75**, 041404(R) (2007); E. H. Hwang and S. Das Sarma, *ibid*. **75**, 205418 (2007); P. K. Pyatkovskiy, J. Phys.: Condens. Matter **21**, 025506 (2009); A. Hill, S. A. Mikhailov, and K. Ziegler, Europhys. Lett. **87**, 27005 (2009); A. Botswick, T. Ohta, Th. Seyller, K. Horn, and E. Rotenberg, Nat. Phys. **3**, 36 (2007).

[18] S. A. Mikhailov and K. Ziegler, Phys. Rev. Lett. **99**, 016803 (2007).

[19] M. Jablan, H. Buljan, and M. Soljačić, Phys. Rev. B **80**, 245435 (2009).

[20] V. Ryzhii, A. Satou, and T. Otsuji, J. Appl. Phys. **101**, 024509 (2007).

[21] V. Ryzhii, M. Ryzhii, and T. Otsuji, J. Appl. Phys. **101**, 083114 (2007); F. Rana, IEEE Trans. Nanotechnol. **7**, 91 (2008).

[22] Yu. V. Bludov, M. I. Vasilevskiy, and N. M. R. Peres, Europhys. Lett. **92**, 68001 (2010).

[23] A. Vakil and N. Engheta, Science **332**, 1291 (2011).

[24] L. Ju, B. Geng, J. Horng, C. Girit, M. Martin, Zh. Hao, H. A. Bechtel, X. Liang, A. Zettl, Y. Ron Shen, and F. Wang, Nat. Nanotechnol. **6**, 630 (2011).

[25] W. L. Barnes, T. W. Preist, S. C. Kitson, and J. R. Sambles, Phys. Rev. B **54**, 6227 (1996); N. Glass, M. Weber, and D. Mills, *ibid*. **29**, 6548 (1984).

[26] H. Yan, X. Li, B. Chandra, G. Tulevski, Y. Wu, M. Freitag, W. Zhu, Ph. Avouris, and F. Xia, Nat. Nanotechnol. **7**, 330 (2012).

[27] U. Fano, Phys. Rev. **124**, 1866 (1961).

[28] A. Christ, T. Zentgraf, J. Kuhl, S. G. Tikhodeev, N. A. Gippius, and H. Giessen, Phys. Rev. B **70**, 125113 (2004); M. V. Rybin, A. B. Khanikaev, M. Inoue, K. B. Samusev, M. J. Steel, G. Yushin, and M. F. Limonov, Phys. Rev. Lett. **103**, 023901 (2009).